修士論文

Structural analysis of the higher-order visual center and the visual projection pathways in the *Drosophila* central brain

キイロショウジョウバエ脳中枢における高次視覚中枢
および視覚系投射神経の構造的解析

四宮　和範

学籍番号：47-56908

指導教員：伊藤　啓

Table of Contents

Abstract	3
Introduction	5
Materials and Methods	8
Results	13
Discussion	25
Acknowledgements	33
References	34
Figures	39
Tables	52

Abstract

Recent neuroanatomical studies on the brain of the *Drosophila melanogaster* have identified various sensory projection pathways to the central brain. As the results of these studies, one neuropile called the ventrolateral protocerebrum (vlpr) turned out to be projected by some of the identified pathways of the visual, olfactory and auditory systems. This region is the only neuropile known so far that receives inputs of three different sensory modalities. The vlpr has been regarded as one of the higher-order visual center so far, since a number of visual information neurons project to this region from the optic lobe, the lower-order visual center. While the structure of the lower-order centers of the sensory systems in the insect brain have been studied extensively, little is known about the mechanisms of sensory processing and integration in the central brain. In this study, with an eye on elucidation of the mechanism of the sensory integration in the future, I firstly analyzed three-dimensional internal structures of the vlpr by immunostaining with a synaptic marker and identified eleven glomeruli and six tracts, which can serve as landmarks in the region. Then, detailed projection areas and directionalities of the thirteen sensory pathways that project to the vlpr were analyzed using GAL4 enhancer-trap system. I found that five of the glomeruli identified in this study were innervated by the visual projection neuron (VPN) pathways from the lobula and that the presynaptic terminals of these pathways reside in the vlpr. The projection pattern of visual projection neurons was also examined by visualizing single

neurons with the flip-out technique, and as a result, the two-dimensional visual topology in the lobula turned out to be conserved to some extent even in the vlpr. This is the first example that anatomically indicates the possibility of conservation of visual planer topology in the central brain.

Introduction

Processing and integration of sensory information obtained from the environment are crucial for the survival of all animals. The central nervous system (CNS) of insects have been studied for more than one hundred years to illustrate the processing mechanisms of sensory information, because an insect's brain have advantages of smaller size and less complexity than most of the vertebrates' brains. At the same time, numerous behavioral experiments and observations of specific behaviors (McGuire et al., 2005; Waddell, 2005) have clearly shown that sensory information is actually integrated in insects' nervous system. Neural circuits that accomplish sensory integration like these, however, have not been clarified so far at all. Neural pathways of the CNS that have been identified using blowfly, silkworm moth, honeybee, locust and so on, have been just confined to low-order sensory pathways and limited types of motorneurons, and virtually nothing is known about higher-order mechanisms of integration.

In this study, I mainly analyzed the configuration of sensory pathways and neurons in the brain of the fruit fly (*Drosophila melanogaster*). Although it has not been so long since *Drosophila* started to be used as a model organism for neuroanatomy, it has a number of advantages for neuroanatomical investigation. Firstly, the size of the brain is even smaller (approx. 800μm in width) than the brains of other insects. Tracing long axons under microscope is relatively easy, since a whole brain can be observed in one viewing field of a microscope. Secondly, the GAL4 enhancer-trap method

(Fig. 1), which enables labeling of specific cells or neurons genetically with reporter proteins, is established. The GAL4 enhancer-trap system requires the implantation of a transcription modulating factor of yeast (GAL4) inserted in a transposon into the genome of a fly. When this fly is crossed with another fly that have an Upstream Activation Sequence (UAS), the target sequence of GAL4, in its genome, then the inserted transgene lying after the UAS sequence is expressed forcedly in the animals of the next generation (Brand and Perrimon, 1993). This method makes morphological analyses of specific pathways/structures highly efficient. Because only Golgi's staining and/or dye injection methods whose staining patterns are hardly reproducible are applicable for identification of neurons in other insects and animals, GAL4-UAS is a significant advantage of *Drosophila*. The method also enables expression of arbitrary genes in specific subsets of the cells.

Recently, description of sensory pathways such as olfactory (Tanaka et al., 2004), visual (Otsuna and Ito, 2006), auditory (Kamikouchi et al., 2006) and gustatory (Gendre et al., 2004; Inoshita and Tanimoto, 2006) systems of *Drosophila* has been dramatically advanced using the GAL4 enhancer-trap system. Some behavioral experiments using the enhancer-trap method also indicate functions on information processing of higher-order areas such as the neuropile called the central complex (Liu et al.).

Applying these backgrounds, in this study, I mainly analyzed the morphology of the sensory neural pathways that project to a neuropile called the ventrolateral protocerebrum (vlpr) to grab a key of the mechanisms of

sensory integration. The vlpr, a neuropile widely conserved through arthropods, is a pair of large neuropiles that are located in the both sides of the anterior-lateral area of the central brain (Fig. 2). Since the region is innervated by many visual projection pathways from the optic lobe, the lower-order processing center of visual information, it has been regarded as one of the higher-order visual centers in the central brain. However, Tanaka et al. (2004) and Kamikouchi et al. (2006) reported that various olfactory and auditory pathways also project to the vlpr. No other neuropiles than the vlpr are identified anatomically to be projected by all of the three modalities of visual, olfactory and auditory systems.

It is rather reasonable to assume that the multimodal information transmitted by these pathways should be integrated in this neuropile. Farther anatomical analyses on the sensory pathways may reveal circuits of sensory integration. In spite of this, the vlpr has hardly been investigated so far both anatomically and functionally. The knowledge on this neuropile is far behind those available on the optic lobe, the antennal lobe and the central complex of which anatomical and functional characteristics have been investigated intensely.

This study aims to describe the internal morphology of the vlpr in detail, as well as to identify the position of projections of the sensory pathways and to reveal the patterns of projection. Then relationship between the confirmed morphologies and their functional properties in sensory processing systems in the *Drosophila* CNS is discussed.

Materials and Methods

Experimental Animals

Flies were raised on standard yeast/cornmeal/agar medium at 25°C under 12hr/12hr of Light/Dark cycle. To apply the heat shock, animals in food vials were placed in a constant-temperature water bath (SJ-10, TAITEC) at 37°C for 30-60 minutes.

Brains of female flies at the age of 5-10 days after eclosion were observed in all experiments. Flies of Canton-Special (CS) strain were used as the wild type. The following transgenic GAL4 enhancer-trap strains (NP series: Yoshihara and Ito, Hayashi et al.) were used for the GAL4-UAS and the flip-out (Basler and Struhl, 1994) techniques. The GAL4 strains *NP1502* and *NP5039* (Otsuna and Ito, 2006) and *201Y* (Yang et al., 1995) were used for labeling the glial tissue, the giant fiber system and the mushroom body, respectively. Thirteen GAL4 strains (see detail for Table 1.) that have been previously identified were used to label visual (Otsuna and Ito, 2006), olfactory (Tanaka et al., 2004 and unpublished data) and auditory (Kamikouchi et al., 2006) pathways.

UAS-reporter strains used were as follows: UAS-*GFP S65T* (T2 strain, gift from Barry Dickson) and UAS-*DsRed S197Y* (C6 strain; Verkhusha et al.) for visualizing general morphology of the *GAL4*-expressing cells. A strain carrying both DsRed and UAS-*neuronal synaptobrevin::GFP* (UAS-*n-syb::GFP*; Ito et al.) for labeling entire neurons (DsRed) and

presynaptic sites (n-syb::GFP) simultaneously. Another strain carrying both DsRed and UAS-*Rdl-HA* (gift from Andreas Prokop), which was expected to visualize postsynaptic sites, was also used.

Fly strain carrying the transgenes Hs-*flp* and UAS>*CD2*, y>*mCD8::GFP* (Wong et al.) was used in the flip-out analysis to generate samples with stained single-neurons.

Dissection and immunostaining of the brains

Animals were anesthetized with carbon dioxide gas and rinsed briefly in ethanol prior to decapitation. Brains were dissected out of the head capsule in phosphate-buffered saline (PBS, pH 7.4 at 25°C). The dissected brains were fixed in 4% formaldehyde in PEM (100 mM PIPES, 2 mM EGTA, 1mM MgSO4, 2 hours at 4°C) and rinsed with 0.5% PBT (0.5% Triton X-100 in PBS) three times for 15 minutes. Samples for immunostaining were rinsed once with 2.0% PBT (2.0% Triton X-100 in PBS) for 30 minutes in addition to this. Samples for immunostaining were subsequently incubated in 10% normal goat serum (Vectastain, Vector Laboratories, Burlingame, CA) in 0.5% PBT for 1 hour, then in a mixture of primary antibodies at 4°C for three days for nc82 antibody and overnight for the other antibodies.

Samples were washed three times for 15 minutes with 0.5% PBT and incubated with a mixture of secondary antibodies at 4°C for two days for the secondary antibody for nc82 and overnight for the others. After three

15-minute rinses with PBT and a 5-minute rinse with PBS, samples were incubated in 50% glycerol in PBS for 2 hours at 4°C, then in 80% glycerol in H2O overnight. Samples were mounted in the same solution on the slides using a layer of 0.2 mm-thick polyvinyl chloride (PVC) electrical insulating tape as a spacer.

Antibodies used in this study were as follows. Rabbit anti-DsRed polyclonal antibody (TAKARA BIO; #632496, 1:1000) to enhance the signal of expressed DsRed. Mouse monoclonal antibody nc82 (gift from E. Buchner and A. Hofbauer, 1:20), mouse anti-Syntaxin antibody (Hybridoma Bank) and mouse BP102 anti-CNS axons (Hybridoma Bank) for labeling neuropiles and identification of internal structures of the vlpr. Rat anti-HA monoclonal antibody (Roche; #11 867 423 001, 1:500) for detection of Rdl-HA. Rat anti-GFP monoclonal antibody (nacalai tesque; #04404-26, 1:1000) and mouse anti-rat CD2 monoclonal antibody (Serotec; #MCA443R, 1:1000) were used to visualize neurons in flip-out experiments. Alexa Fluor 647-conjugated anti-mouse IgG (Molecular Probes; #A-21236, 1:250), Cy3-conjugated anti-rabbit IgG (Jackson ImmunoResearch, West Grove, PA; #111-165-144, 1:300), Cy3-conjugated anti-mouse IgG (Jackson ImmunoResearch; # 115-165-146, 1:300) and Alexa Fluor 448-conjugated anti-rat IgG (Molecular Probes; #A-11006, 1:250) were used as second antibodies.

Identification of internal structures of the ventrolateral

protocerebrum

The enhancer-trap strain *NP1502* and the UAS-*GFP S65T* (T2) strain were used to visualize glial structures in the brain. In the same time, nc82 antibody, a marker of the active zone of synapse, was applied to identify detailed internal structures of the neuropiles.

Confocal serial optical sections at 0.9-1.8 μ m intervals were taken with LSM 510 confocal microscopes (Carl Zeiss, Germany) and water-immersion 40× Plan-Apochromat objective lenses (NA 1.2). The whole-mount brain samples were scanned from the anterior side, because the ventrolateral protocerebrum is located in the anterior region of the brain.

Visualization of labeled cells and image processing

To visualize the morphology of the neurons of interest more clearly, unwanted cells and signals were removed from the sequential images of brains. For this process, a series of pictures taken with Zeiss LSM 510 were exported as a Multi-page TIFF-format file. The TIFF file was imported to ImageReady software (Adobe), where each page is assigned to a distinct layer, and converted to a Photoshop PSD-format file. The additional signals other than the fibers and cell bodies that belong to the neurons of interest were carefully selected in each layer and painted black with PhotoShop CS software (Adobe Systems). The resulting images, where only the signals of

the intended neurons remain, were exported in TIFF-format.

Three-dimensional (3D) reconstruction and remodeling of the neurons

The confocal datasets were subjected to 3D reconstruction. The Imaris 2.7 software (BitPlane) running on Silicon Graphics Octane2 workstations was used for general reconstruction (Figs. 5-7, 9 and 10). Imaris 2.7 recruits the "ray-tracing" algorithm, which provides better quality of images of individual neurons than other methods such as maximum intensity, averaging or iso-surface extraction. Direction of the projection can be adjusted upon reconstruction; i.e. reconstructed images of ventral view can be generated from the images taken from the anterior side.

The 3D remodeling software Amira3.1.1 (Mercury Inc.) was applied to describe areas or structures (Figs. 2 and 4) and to perform standardization of single neurons (Fig. 13). To visualize remodeled images, the signals of intended structures or neurons in every section in a serial image have to be "painted" more or less manually on the software, so that additional signals are excluded from remodeled images. Once the painting is completed, transparency or angle of the objects can be changed arbitrarily.

Results

Identification of the internal structures in the vlpr

In the insect brain, there exist a number of neural structures called neuropiles, which are isolated by cell body layers from each other. In the *Drosophila* brain, the boundaries and the relative location of the neuropiles were previously defined (Otsuna and Ito, 2006). In some neuropiles, characteristic internal structures that are closely related to their functions have also been identified, such as layers in the neuropiles in the optic lobe, glomeruli in the antennal lobe and the layered structure of the mushroom body. However, in most parts of the brain, only few prominent internal structures are known, because systematic and comprehensive descriptions of these regions have rarely been performed. Identifying typical structures is also necessary for determination of projecting areas of the sensory pathways in the neuropile, because they can be determined by relative coordination against “landmarks” that do not depend on individual variability of the brain size.

In order to visualize the internal structures of the vlpr, firstly I tried to observe the brain using whole-mount immunostaining with so-called neuropile markers. I used nc82, anti-syntaxin and BP102 antibodies and compared the labeling patterns. The best signal-to-noise ratio and contrast of the image were obtained with the nc82 antibody. Furthermore, in the vlpr labeled with nc82, characteristic and reproducible six cylinder-like areas and

eleven structures that were labeled more strongly than the surrounding areas were observed. These eleven structures were not observed when anti-syntaxin or BP102 antibodies were used for immunostaining. Thus, in the following experiments I used nc82 antibody for background staining. To observe these structures in more detail, I crossed a GAL4 strain *NP1502*, which specifically labels glial cells, with the reporter strain UAS-*GFP S65T* (T2), dissected the brain of the next generation and immunostained with nc82 antibody.

The cylinder-like areas not labeled with nc82 antibody represent the tracts, which are the bundles of axons that lack synapses. These tracts were lined with glial processes (Fig. 3C). Tracts are distributed mainly in the anterior half of the vlpr (Fig. 4D). The six identified tracts are named as TR1 to TR6 in this study as indicated in Fig. 4C and 4D. Among them, TR3 turned out to be a part of the outer antenno-cerebral tract (oACT), a tract that connects the antennal lobe and the neuropiles in the superior protocerebrum through the vlpr.

The structures strongly labeled with nc82 antibody were also surrounded by thin glial processes (Figs. 3C and 3D). This feature is similar to that of the glomeruli in the antennal lobe, the first-order olfactory center (Figs. 3A and 3B). Consequently, I defined these structures in the vlpr as glomeruli (GL) and named them as GL1 to GL11. The spatial arrangements of the tracts and glomeruli are indicated in Fig. 4. All of the glomeruli were located in the posterior half of the vlpr. No direct relationship between the locations of the glomeruli and the tracts was found.

In the brain of the blowfly (*Calliphoridae*), structures called optic glomeruli, which are located in the protocerebrum including the vlpr, have been reported (Strausfeld, 1976; Strausfeld and Okamura, 2007). These are the terminals of visual projection neuron pathways from the optic lobe. The following experiments revealed that at least some of the glomeruli identified in this study may correspond to the optic glomeruli, because they turned out to contain the terminals of the visual projection neurons.

Projection sites of the visual pathways in the vlpr

Previous studies identified thirteen sensory pathways (9 visual, 3 olfactory, 1 auditory, see Table 1.) that project to the vlpr. What described in these studies were mainly the morphology and the positions of the terminals in the lower-order centers, including those in the optic lobe (visual), the antennal lobe and the lateral horn (olfactory) and the Johnston's organ (auditory). However, the positions of their terminals in the vlpr, the higher-order region, have not been identified in detail. In this study, I therefore visualized these pathways using GAL4 enhancer trap strains with background immunostaining with nc82 antibody to determine the detailed projecting areas in the vlpr.

Firstly I used DsRed S197Y and n-syb::GFP as reporter proteins. The former labels cell bodies and entire axons, while the latter is specifically localized in the presynaptic terminals. The directionality of information of

specific pathways can be assumed by localization of n-syb::GFP. Results are shown in Figs. 5-7.

Figs. 5 and 6 show the structure of the nine visual projection neuron (VPN) pathways arising from the lobula, the higher-order neuropile in the optic lobe. Five of them (Fig. 5) are the pathways called the lobula-specific columnar-type pathways (LC pathways). Each LC pathway consists of a relatively large number of neurons (approx. 30-330 cells per pathway). The terminals of each neuron of the LC pathways in the lobula form columnar organization called the visual cartridge. The relative position of each visual cartridge reflects the position of the associated ommatidia on the retina and therefore the position in the visual field. The terminals of each LC pathway accurately corresponded to one of the glomeruli identified in the previous section, and n-syb::GFP was observed in all of these terminals. This result indicates that at least five (GL2, 5, 7, 10, 11) glomeruli that are innervated by the LC pathways may correspond to the optic glomeruli previously reported in the brain of the blowfly.

Among the five LC pathways, the LC4 pathway is likely to have synaptic contact with a previously identified descending neuron, the giant fiber, at the glomerulus GL10. The giant fiber is a pair of single-neuronal pathways to the thoracic ganglia and mediates startle response (Milde and Strausfeld, 1990). This pathway is known to be connected with a VPN pathway called the colA at the lateral protocerebrum (Hausen and Strausfeld, 1980; Strausfeld, 1980). Otsuna and Ito (2006) pointed out morphological similarities between the LC4 and the colA, but did not yet conclude that they

were the same pathway. It is also known that there exist both chemical and electrical synapses at the connection of the two pathways (Strausfeld and Bassemir, 1983). In this study I used the enhancer-trap line of *NP5039* to label the giant fiber system and observed the projection site of the giant fiber (Fig. 9). One of the terminals was confirmed to be in the GL10, which also contains the presynaptic terminals of the LC4 pathway. This clearly indicates that the LC4 is the same pathway as the previously described colA.

The other type of the visual pathways projecting to the vlpr called the lobula-specific tangential/tree-like pathways (LT pathways, Fig. 6). These pathways, contrary to the LC pathways, consist of relatively small numbers of neurons (1-4 cells per pathway) and their terminals in the lobula form tangential or tree-like organizations that are perpendicular to the visual cartridges. In the vlpr, the terminals of these pathways were sparse and clearly distinguishable from condensed terminals of the LC pathways. n-syb::GFP were observed at all the terminals of the LT pathways in the vlpr, as well as in specific layers (lo3 and lo4) in the lobula in case of the LT11 (Otsuna and Ito, 2006).

Projection sites of the olfactory pathways in the vlpr

Next I studied the terminals of the olfactory pathways (Figs. 7A-7F). The oACT (outer antenno-cerebral tract) and the PN (posterior neuron) are the second-order pathways that connect the antennal lobe (AL), the

first-order olfactory center, and other regions of the brain including the vlpr (see Table 1), whereas the LHN (lateral horn neuron) is a third-order pathway that connect the lateral horn (LH), one of the second-order olfactory centers, and the vlpr. The terminals of these three pathways in the vlpr were sparse. n-syb::GFP was observed in the terminals in the vlpr in the oACT and the LHN, whereas it was not observed at all in the PN. This result indicates that the PN may have postsynapses (input synapses) in the vlpr and may be an output pathway to other neuropiles in the brain or to the cervical connect that leads to the thoracic ganglia.

Projection sites of the auditory pathway in the vlpr

The JON-AD (Figs. 7G and 7H) is a branch of the axons of auditory sensory neurons whose cell bodies lie in the Johnston's organ, the mechanosensory receptor in the antennae. This means that the JON-AD is one of the primary pathways of the auditory system. The JON-AD is only known auditory pathway that projects to the vlpr. This pathway projects to the most ventral area of the vlpr, where n-syb::GFP was localized. Its terminal was rod-shaped, and the localization of n-syb::GFP looked rather condensed, this region, however, does not correspond to any of the glomeruli identified with nc82 antibody.

Projection mapping of the terminals of the sensory pathway in the vlpr

The projection target regions of the thirteen sensory pathways were mapped on the vlpr (Fig. 8A and 8B). The projection areas of each modality were almost exclusive with each other.

All of the visual LC pathways projected to the posterior half of the vlpr, because their projection targets were each of the glomeruli. Among the visual LT pathways, only the LT1 projected to the anterior half, whereas the others projected to the posterior region. The projection areas of the LC pathways and the LT pathways were significantly overlapped in the posterior region. The projection areas of the olfactory pathways, on the other hand, were mainly positioned in the anterior half except for the oACT, which have presynaptic sites both in the anterior and the posterior half. The projection areas of the olfactory pathways were also peculiar that all of them were observed only in the medial region. The terminal of the auditory pathway, the JON-AD, was in the anterior and the most ventral region and it did not overlap with any of the terminals of the other pathways.

The most posterior region of the terminal of the oACT looked partially overlapped with that of the LT10 (Figs. 8C and 8D). This was the only one area where neurons of different modalities may project overlappingly. To determine if there are synapses between the neurons of the two modalities, crossing of the two strains that label each pathway would be required.

Probation of Rdl-HA as a postsynaptic marker

To investigate the directionalities of the pathways accurately and in more detail, a postsynaptic marker is demanded to be used in conjunction with n-syb::GFP. However, no good postsynaptic markers have been available for *Drosophila*. GABA (gamma-aminobutyric acid) acts as the inhibitory neurotransmitter in synaptic transmission, and Rdl (resistant to dieldrin) is a subunit of GABA receptor. Rdl is known to be expressed in most of the neurons in the *Drosophila* brain (Aronstein and Ffrench-Constant, 1995; Okada, unpublished observation). Since a fly strain that expresses Rdl with an HA tag (UAS-*Rdl-HA*) was available but not confirmed as a reliable postsynaptic marker, so I verified the usability of the strain before using it as a postsynaptic marker. For this purpose, I applied a GAL4 enhancer-trap line *201Y*, which labels the neurons of the mushroom body (MB). Figs. 10A and 10B show the mushroom body with visualized with DsRed and n-syb::GFP driven by *201Y*, whereas Figs. 10C and 10D with DsRed and Rdl-HA. n-syb::GFP was localized only in the lobes but not in the calyx of the MB, whereas Rdl-HA was observed both at lobes and calyx.

I also tried preliminarily to cross Rdl-HA strain with the GAL4 lines labeling the thirteen sensory pathways and observed its distribution. For the first trial, Rdl-HA was detected only in the LC (visual) pathways and the JON-AD (auditory) pathway. The regions where Rdl-HA was observed are shown in Table 1. In the LC pathways, Rdl-HA was observed in all of the five

glomeruli in the vlpr (the localization pattern of Rdl-HA in the LC4 pathway is displayed in Figs. 10E and 10F). This means that both presynaptic marker (n-syb::GFP) and postsynaptic marker (Rdl-HA) were localized at the same glomeruli. In some of the LC pathways, Rdl-HA was also observed in the lobula in a layered manner. This result is consistent with the fact that arborization within the layers in the lobula of LC pathways shows dendritic characteristics (Fischbach and Dittrich, 1989; Otsuna and Ito, 2006). The localization pattern of Rdl-HA in the JON-AD was also consistent with previous observations of JON (Kamikouchi, unpublished data). So far I couldn't detect specific localization of Rdl-HA in specific subareas of the LC pathways at lobula, as well as in the LT pathways and the olfactory pathways.

Distribution of the single neurons of the visual projection pathway in the vlpr

Although many sensory pathways that project to the central brain have been identified, detailed morphologies of most of their terminals are not yet well known. Whereas it is relatively easy to analyze the morphology and projection pattern of pathways that consist of single or only a few neurons, it is much harder to analyze the pathways that consist of large numbers of neurons. The visual LC pathways are the representatives of such type. Contrary to the LT pathways, the LC pathways consist of many (approx.

30-330/pathway) neurons. It is known that the two-dimensional topological information of the visual field received in the retina is conserved throughout the optic lobe, because the visual cartridges of all the neuropiles in the optic lobe (the lamina, the medulla and the lobula/the lobula plate) are connected specifically by columnar neurons. Such topological information cannot be transferred to the central brain via LT pathways, whose receptive dendrites cover all cartridges of the lobula. In LC pathways, on the other hand, each component neuron can mediate information about different areas of the visual field, because one neuron has dendrites only across a small number of visual cartridges. This suggests that the LC pathway may transmit two-dimensional topological information to the central brain. The neurons of the LC pathways, however, form dense bundles of axons, and their terminals form a glomerular structure with highly condensed synapses. It is therefore almost impossible to trace each axon and to distinguish whether the topological information is intermingled within the glomerulus.

To solve this problem, I applied the "flip-out" method (Wong et al., 2002; Marin et al., 2002) to visualize single neurons out of those labeled by a particular GAL4 strain and determined the relative positions of each axon against the bundle of the whole axons of the pathways. The overview of the flip-out method is shown in Fig. 11, and the scheme of the location determination is shown in Fig. 12A. Using this method, I first analyzed the LC4 pathway as a typical example of the LC pathways. In the pathway, the bundle becomes the narrowest at the area between the lobula and the vlpr. I termed this area as "neck" of the pathway. The region between the neck and

the glomerulus (GL10), where no n-syb::GFP localization is observed (region from the neck to the point of 34.5±1.9% from the neck; n=8, data not shown) was defined as the "fascicle". Using Zeiss LSM Image Browser, I next measured the relative position of the axon of single neuron against contour of the entire bundle in the sagittal cross-sectioned image. Every specimen was measured at four points; at the lobula, the point of 30% from the neck of fascicle, 70% from the neck of fascicle, and at the middle point of the glomerulus GL10. Since one axon bifurcates into several branches in the glomerulus, the thickest fiber in the GL10 was measured.

Results of this experiment show that the topology in the dorso-ventral (D-V) axis is inverted between the lobula and 30% of the fascicle. The average axis of inversion is displayed in Fig. 12B (θ=-13.75°). This means a kind of chiasm should exist at the neck area. Figs. 12C and 12D show that the relative positions of axon fiber are rotated in a clockwise direction between 30% and 70% of the fascicle (average rotation angle; θ=-47.6±28.8°), and between 70% of the fascicle and the middle of the glomerulus (θ=-76.8±49.3°). These results suggest that the single axons in the LC4 pathway are oriented in its bundle according to the area of their dendritic field in the lobula, but not disorderly.

To confirm these results three-dimensionally, I next compared the morphology of five single LC4 neurons obtained from five independent specimens. Amira 3.1.1 was utilized to perform this operation. Since the size, orientation and the overall morphology of the specimens are not identical between different samples, three-dimensional images of the five neurons

were standardized into one “standard brain” format using the Virtual Insect Brain protocol described by Jenett and colleagues (2006) (Fig. 13). From these images, D-V inversion at the neck area, twisted arrangement in the fascicle, and the topological conservation at the projection pathway to the glomerulus can be seen clearly. However, complicated tangled bifurcations of each axon at the distal area of the glomerulus clearly shown in the figures mean that the projection areas of single neurons in the glomerulus should be overlapped to a significant extent.

Discussion

Internal structures in the vlpr

In this study, I identified eleven glomeruli and six tracts in the vlpr with the immunostaining with nc82 antibody. Since nc82 antibody is an active zone marker and the glomeruli were labeled strongly with it, synaptic density should be higher in the glomeruli than in the surrounding area. The optic glomeruli have been reported by Strausfeld and colleagues in this region of the blowfly (Strausfeld, 1976; Strausfeld and Okamura, 2007), however, all of them were identified as the terminals of the visual projection pathways. This is the first study that determined internal structures from the angle of pure morphology visualized with the synaptic marker, leaving from certain modalities or pathways. This study also shows the first perspective that not only the olfactory glomeruli in the antennal lobe and the optic glomeruli but glomeruli processing other types of information may exist in the brain.

Although no obvious structures can be observed with immunostaining with anti-syntaxin or bp102 antibody, other glomeruli that were not visualized with nc82 may be found in the vlpr when other antibodies or visualization methods are applied, so it should be noted that not all internal structures in the vlpr are visible with nc82 staining.

The volumes and the shapes of the glomeruli varied widely from each other. The shapes of the glomeruli such as GL1-5, GL10 and GL11 were more

or less cylinder-like, whereas GL6 and GL7 looked more rounded than the others (see Figs. 4C and 4D). This is a significant difference between the glomeruli in the vlpr and the antennal lobe, as almost all of the glomeruli in the antennal lobe are spherical. The morphology of the glial processes around the glomeruli is also different between them. The glial processes in the antennal lobe are relatively thick and isolate the glomeruli from others, whereas those around the vlpr glomeruli look much thinner.

Since at least five of the eleven identified glomeruli were projected by the VPNs, they are considered as the equivalents of some of the optic glomeruli in the lateral protocerebrum. But since positions of the optic glomeruli were not described unambiguously in the previous studies, it is almost impossible to correlate each of them with the glomerulus identified in this study.

No VPNs were found that project to the other six glomeruli (GL1, 3, 4, 6, 8 and 9). Some of these glomeruli might be projected by yet unidentified VPNs. Other types of pathways, such as unknown sensory pathways of other modalities, pathways that connecting to higher-order integration centers or pathways to the motor output systems (i.e. the giant fiber) might also project to them. Some vlpr-intrinsic neurons that project to the glomeruli have also been found (data not shown) in my screening of other GAL4 enhancer-trap lines.

Projection areas of the sensory information pathways in the vlpr

The target areas of the sensory pathways of different modalities turned out to be segregated (Fig. 8). This means that sensory information is not very likely to be transmitted directly to each other. Thus, in the vlpr, integration of sensory information should be accomplished mainly by higher-order neurons in the vlpr, which would interconnect different areas. Also, the sensory information is likely to be processed in parallel at the primary step within the vlpr. Even the information of the same modality may be subdivided into more specific information and processed independently. The visual information, for example, should be divided in the optic lobe and conveyed in parallel to the five glomeruli by the LC pathways and the posterior area of the vlpr by the four LT pathways.

The orders of the sensory pathways analyzed in this study are limited to certain levels (visual: third- or fourth-order pathways, olfactory: second- or third-order pathways, auditory: first-order pathways). Farther description and identification of sensory pathways may reveal new connections to the vlpr, such as auditory secondary pathways or gustatory pathways of other levels.

Among the olfactory pathways analyzed in this study, the oACT and the PN are the second-order pathways and the LHN is the third-order pathway. The projection areas of these three pathways, interestingly, lie close to each other. This suggests that the olfactory information may be processed in a unified manner in one area in the vlpr regardless of the difference of the order of the pathways.

Identification of presynaptic and postsynaptic sites

In this study, I labeled presynaptic sites using n-syb::GFP. n-syb::GFP was confirmed experimentally to localize in the presynaptic terminals when it was expressed (Ito et al., 1998). This has become a powerful tool for assuming the directionality of information in neurons or pathways. Postsynaptic sites are expected to exist at terminals where n-syb::GFP is not localized. However, there has been no reasonable method to detect them. Identification of postsynaptic sites has been relied mainly on observation by electron microscopy. One of the reasons of this difficulty on detecting the postsynapses is due to the various types of postsynapses that reflect the variety of transmitter molecules.

This time I preliminarily used the Rdl-HA fusion protein as a candidate molecule of a postsynaptic marker. In the mushroom body, Rdl-HA was localized not only in the lobes but also at the calyx where n-syb::GFP was not detected. This means that the output synapses (presynapses) are localized only in the lobes. Rdl-HA was also detected in the terminals of some LC pathways in the lobula as well as in the glomeruli. The localization of both Rdl-HA and n-syb::GFP in the vlpr glomeruli and mushroom body lobes might indicate the existence of “synapse-on-synapse” structures which are possibly involved in the lateral inhibition mechanism. Expression of Rdl-HA was not detected at all in the LT pathways and the olfactory pathways. This may be caused by the poor quality of immunostaining against Rdl-HA. The

condition of immunostaining to these strains should be reexamined.

These results, however, do not yet prove that Rdl-HA works as a genuine postsynaptic marker, because Rdl-HA was detected in all the terminals where n-syb::GFP was also localized. Since Rdl-HA was not detected in the axons, it is considered to be localized at least in the synapses, though it is still unclear whether it is accumulated both in the pre- and the postsynaptic terminals. To prove that Rdl-HA surely labels postsynapses, it is necessary to express both a presynaptic marker and Rdl-HA simultaneously in the same neuron and observe synaptic sites in high magnification to see whether the localizations of the two markers do not completely overlap.

Organization of the visual pathways to the vlpr

Among visual pathways, a single tangential-type neuron covers a broad area of the visual field in the lobula. This structure is suitable for conveying information about global areas of the visual field, such as the ambient brightness, movement of the background scenery, and so on. On the other hand, this kind of neuron is therefore not likely to transmit information about specific areas of the visual field, such as the movement of the objects. In contrast, a neuron of the columnar-type pathways is not likely to connect broad areas, because a single neuron extends its arborization only in a small region of the lobula. Thus morphology and the information likely to be transmitted would be significantly different between these two types of

neurons.

Determination of the projection sites in this study revealed that each of the five LC pathways project to one of the glomeruli, while all the LT pathways project to an overlapping area of the vlpr sparsely. This is also consistent with observations of twelve columnar and twenty three tangential/tree-like pathways other than the lobula-specific pathways to the vlpr (Otsuna and Ito, 2006; Otsuna, unpublished data). This fact strongly suggests that the information processing patterns differ depending on types of information originated from the morphologies of the VPNs within the optic lobe.

An LC pathway possibly conveys topological information to the central brain. Structural analysis of the LC4 pathway using the single-cell labeling method (Fig. 11-13) actually showed the topologically conserved projection between the lobula and the GL10, the presynaptic terminal of the LC4. Although the projecting area of each axon overlap considerably each other in the GL10, two-dimensional information of the visual field is possibly transferred to the central brain with its topology conserved, even if the resolution might get much lower.

Although the structures of the other glomeruli projected by the LC pathways are not yet analyzed in detail, preliminary results of the single-neuron experiments on these glomeruli suggest that the internal organizations of the fibers may be different by glomeruli. The axons of the neurons of LC12 pathway looked less regularly orientated than the LC4 in the glomerulus (GL7). The topological information would not be conserved at

the glomeruli if the internal organization of it turned out to be irregular. More accurate orientation pattern of the fibers in the glomeruli should be clarified by applying the same method to this time on the other LC pathways.

This study also revealed an inverted projection pattern along the D-V axis at the “neck” area of the projecting pathway of the LC4. This is the first instance of this kind of structures found within the central brain. Chiasms have been known to exist between the neuropiles of the optic lobe in the insect brains. These are structurally different from that of the LC4, because A-P axes rather than the D-V axes are inverted in these cases. The other LC pathways should be verified with the same method whether they also have structures like this though the functions of chiasm on visual information processing are still not clear.

Description of the neural pathways and the network model

To study the mechanisms of the sensory information processing more comprehensively, it is crucial to construct a global network model of the information pathways that extends the wider brain areas. The information about the sensory projection pathways revealed in this study is still far insufficient to construct such a model. The higher-order pathways that receive the sensory information conveyed to the vlpr, first of all, should be identified. Moreover, the identification of pathways, which have been

performed so far to identify pathways in each modality, should be performed in a high-throughput manner and also extended to the whole brain. To promote this scheme, the huge amount of accumulated data of expression pattern of the GAL4 enhancer-trap strains in the laboratories engaged in neuroanatomy, including ours, are required to be utilized effectively. It will be expected to construct the connectivity map of the sensory information processing in the brain areas or the neuropiles by analyzing the whole data comprehensively, so that the flow of the information processing can be traced on the map. By feedbacking the knowledge obtained by physiological experiments, such as the calcium live imaging, electrophysiology or behavioral experiments, to the network model, it is considered to become more sophisticated.

Acknowledgements

I would like to express my appreciation for supervision and the constant supports by Prof. Dr. Kei Ito. I deeply appreciate Dr. Hideo Otsuna for data on the visual system, constant and intense discussions and both technical and theoretical tutorships. I also express my appreciation to Dr. Arnim Jenett for his tutorship on standardization of brains. I would like to thank Drs. Nobuaki K. Tanaka and Azusa Kamikouchi for the data and advices on the olfactory system and the auditory system, respectively. I thank all the members in the Ito laboratory for thought-provocative discussions and encouragements throughout the course of this research.

References

Aronstein K and Ffrench-Constant R. (1995) Immunocytochemistry of a novel GABA receptor subunit Rdl in *Drosophila melanogaster*. Invert. Neurosci. 1:25-31

Basler K and Struhl G. (1994) Compartment boundaries and the control of *Drosophila* limb pattern by hedgehog protein. Nature 368:208-214

Brand AH and Perrimon N. (1993) Targeted gene expression as a means of altering cell fates and generating dominant phenotypes. Development. 118:401-415

Fayyazuddin A, Zaheer MA, Hiesinger PR and Bellen HJ (2006) The Nicotinic Acetylcholine Receptor Dα7 Is Required for an Escape Behavior in *Drosophila*. PLoS Biol. 4:420-432

Fischbach KF and Dittrich APM. (1989) The optic lobe of *Drosophila melanogaster*. I. A Golgi analysis of wild-type structure. Cell Tissue Res. 258:441-475

Gendre N, Luer K, Friche S, Grillenzoni N, Ramaekers A, Technau GM and Stocker RF. (2004) Integration of complex larval chemosensory organs into the adult nervous system of *Drosophila*. Development. 131:83-92

Guo J and Guo A. (2005) Crossmodal Interactions Between Olfactory and Visual Learning in *Drosophila*. Science 309:307-310

Hausen K and Strausfeld NJ. (1980) Sexually dimorphic interneuron arrangements in the fly visual system. Proc. R. Soc. [B] 208:57-71

Inoshita T and Tanimura T. (2006) Cellular identification of water gustatory receptor neurons and their central projection pattern in *Drosophila*. Proc. Nat. Acad. Sci. 103:1094-1099

Ito K, Suzuki K, Estes P, Ramaswami M, Yamamoto D and Strausfeld NJ. (1998) The organization of extrinsic neurons and their implications in the functional roles of the mushroom bodies in *Drosophila melanogaster* Meigen. Learn Mem. 5:52–77

Jenett A, Schindelin JE and Heisenberg M. (2006) The Virtual Insect Brain protocol: creating and comparing standardized neuroanatomy. BMC Bioinform. 7:544-555

Kamikouchi A, Shimada T and Ito K. (2006) Comprehensive Classification of the Auditory Sensory Projections in the Brain of the Fruit Fly *Drosophila melanogaster*. J. Comp. Neurol. 499:317-356

Liu G, Seiler H, Wen A, Zars T, Ito K, Wolf R, Heisenberg M and Liu L.

(2006) Distinct memory traces for two visual features in the *Drosophila* brain. Nature 439:551-556

Marin EC, Jefferis GSXE, Komiyama T, Zhu H and Luo L. (2002) Representation of the Glomerular Olfactory Map in the *Drosophila* Brain. Cell. 109:243-255

McGuire SE, Deshaver M and Davis RL. (2005) Thirty years of olfactory learning and memory research in *Drosophila melanogaster*. Prog. Neurobiol. 76:328–347

Milde JJ and Strausfeld NJ. (1990) Cluster organization and response characteristics of the giant fiber pathway of the blowfly Calliphora erythrocephala. J. Comp. Neurol. 294:59-75

Otsuna H and Ito K. (2006) Systematic Analysis of the Visual Projection Neurons of *Drosophila melanogaster*. I. Lobula-Specific Pathways. J. Comp. Neurol. 497:928-958

Seeger M, Tear G, Ferres-Marco D and Goodman CS. (1993) Mutations Affecting Growth Cone Guidance in *Drosophila*: Genes Necessary for Guidance toward or away from the Midline. Neuron. 10:409-426

Shanbhag SR and Singh RN (1992) Functional implications of the

projections of neurons from individual labellar sensillum of *Drosophila melanogaster* as revealed by neuronal-marker horseradish peroxidase. Cell Tissue Res. 267:237-282

Strausfeld NJ and Bassemir UK (1983) Cobalt-coupled neurons of a giant fibre system in Diptera. J. Neurocytol. 12:971-991

Strausfeld NJ and Okamura JY. (2007) Visual System of Calliphorid Flies: Organization of Optic Glomeruli and Their Lobula Complex Efferents. J. Comp. Neurol. 500:166-188

Strausfeld NJ. [1] (1976) Atlas of an Insect Brain. Berlin: Springer

Strausfeld NJ. [2] (1980) Male and female visual neurons in dipterous insects. Nature 283:381-3

Tanaka NK, Awasaki T, Shimada T and Ito K. (2004) Integration of Chemosensory Pathways in the Second-Order Olfactory Centers. Curr. Biol. 14:449-457

Verkhusha VV, Otsuna H, Awasaki T, Oda H, Tsukita S and Ito K. (2001) An Enhanced Mutant of Red Fluorescent Protein DsRed for Double Labeling and Developmental Timer of Neural Fiber Bundle Formation. J. Biol. Chem. 276(32):29621–29624

Waddell S. (2005) Courtship Learning: Scent of a Woman. Curr. Biol. 15:R88-R90

Wong AM, Wang JW and Axel R. (2002) Spatial Representation of the Glomerular Map in the *Drosophila* Protocerebrum. Cell. 109:229-241

Yang MY, Armstrong JD, Vilinsky I, Strausfeld NJ and Kaiser K. (1995) Subdivision of the *Drosophila* mushroom bodies by enhancer-trap expression patterns. Neuron. 15:45-54

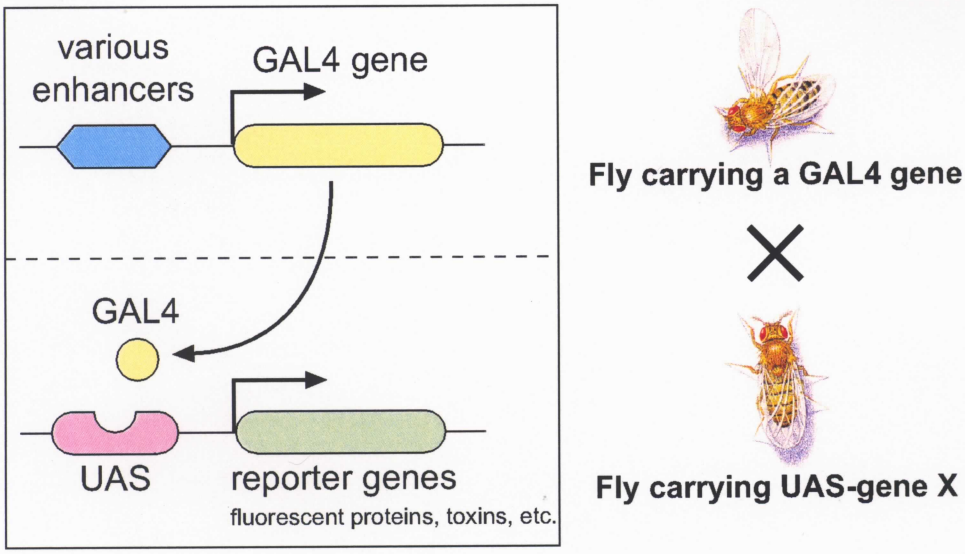

Figure 1. The GAL4-UAS system.

The GAL4 enhancer-trap strains and the GAL4-UAS system is applied for forced expression of foreign genes in *Drosophila* individuals. GAL4 is a transcription modulating factor of yeast. GAL4 gene is integrated into the *Drosophila* genome using a transposon. Translation of GAL4 gene is controlled by enhancers that lie near its insertion point ("enhancer-trap"). Thus, GAL4 gene is expressed in different subsets of cells in strains according to the different insertion sites. When a fly carrying a GAL4 gene is crossed with a fly carrying a reporter gene lying downstream of the Upstream Activation Sequence (UAS), the target sequence of GAL4 protein, the reporter gene begins to be translated only in the specific subset of cells where GAL4 is expressed. Reporter genes can be fluorescent proteins (GFP, DsRed, etc.), other cell markers, or effecter genes such as the toxic gene that inhibit transmission at synapses.

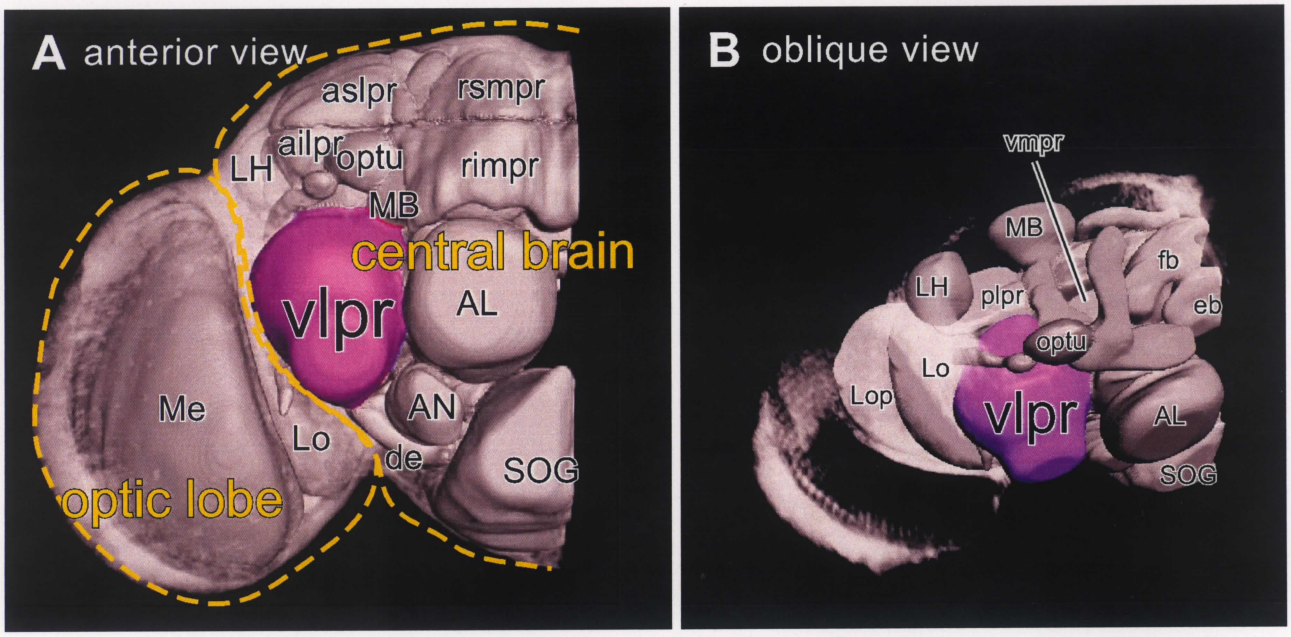

Figure 2. Three-dimensional images of the *Drosophila* brain and location of the vlpr.

The ventrolateral protocerebrum (vlpr) is located at the anterior and lateralmost part of the central brain. The vlpr has the biggest volume in the neuropiles in the central brain. There exists a cell body layer between the vlpr and the optic lobe, whereas the neuropile structure continues to the anterior inferiorlateral protocerebrum (ailpr), the posterolateral protocerebrum (plpr), the deutocerebrum and the ventromedial protocerebrum (vmpr). The images were modified from the figures in Otsuna and Ito (2006).

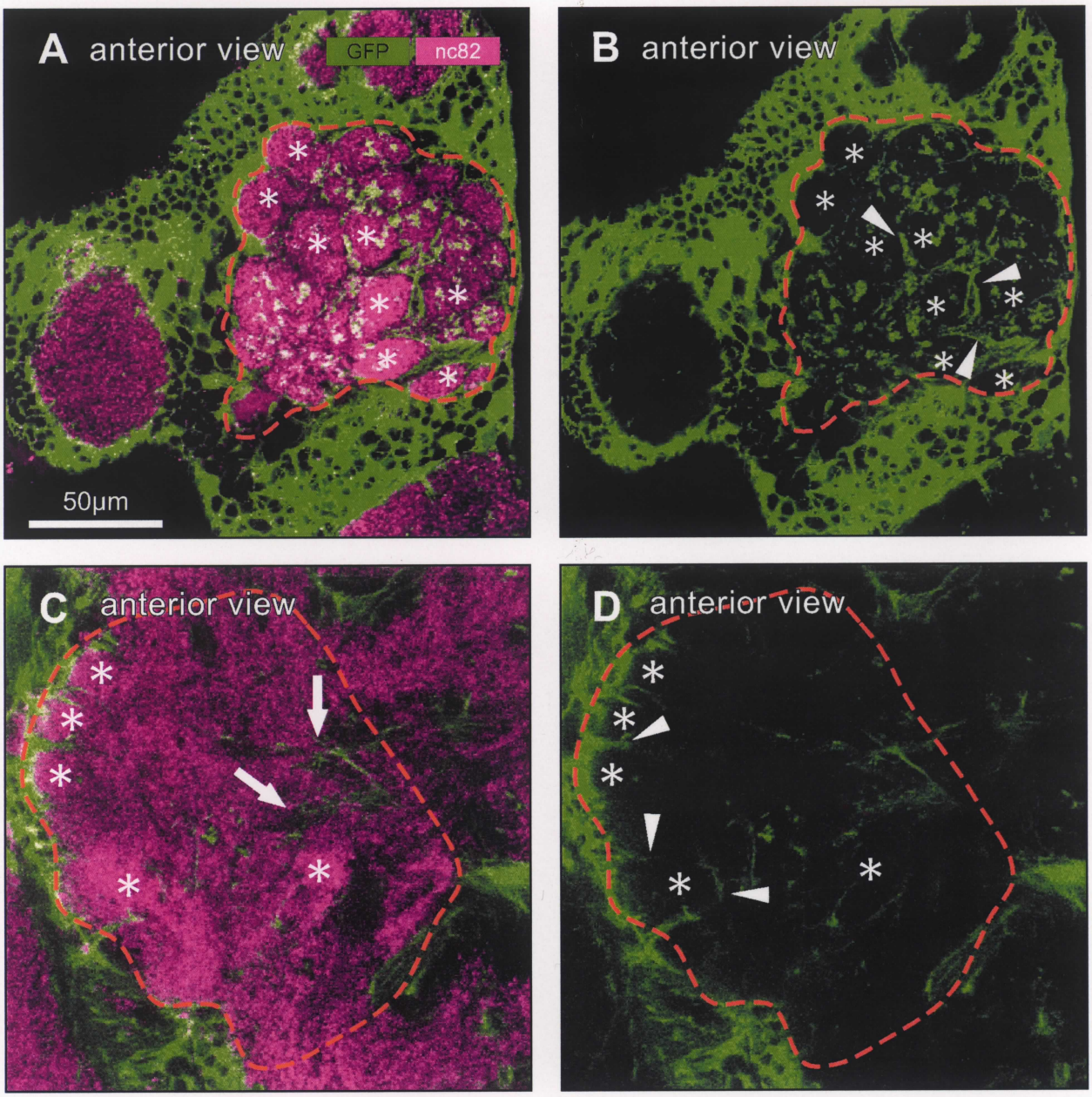

Figure 3. Comparison of internal structures between the antennal lobe and the vlpr.

The antennal lobe (A, B) and the vlpr (C, D) stained with nc82 antibody (purple), a synaptic marker, and GFP::T2 (green) driven by NP1502, a glial tissue-specific GAL4 line. The same parts of the brain are indicated in A, B and in C, D, respectively. Both synapses and glial tissue are displayed in A and C, while only glial tissue is shown in B and D. Olfactory glomeruli are distinguishable in A, and they are surrounded with glial processes as indicated in B. In the vlpr (C, D), similar structure stained strongly with nc82 antibody are found. They are also called glomeruli in this study. Parts of the tracts (arrows), which lack synapses, are also visible in C. Asterisks: representative glomeruli, arrowheads: glial processes around glomeruli, dashed red lines: contours of the neuropiles.

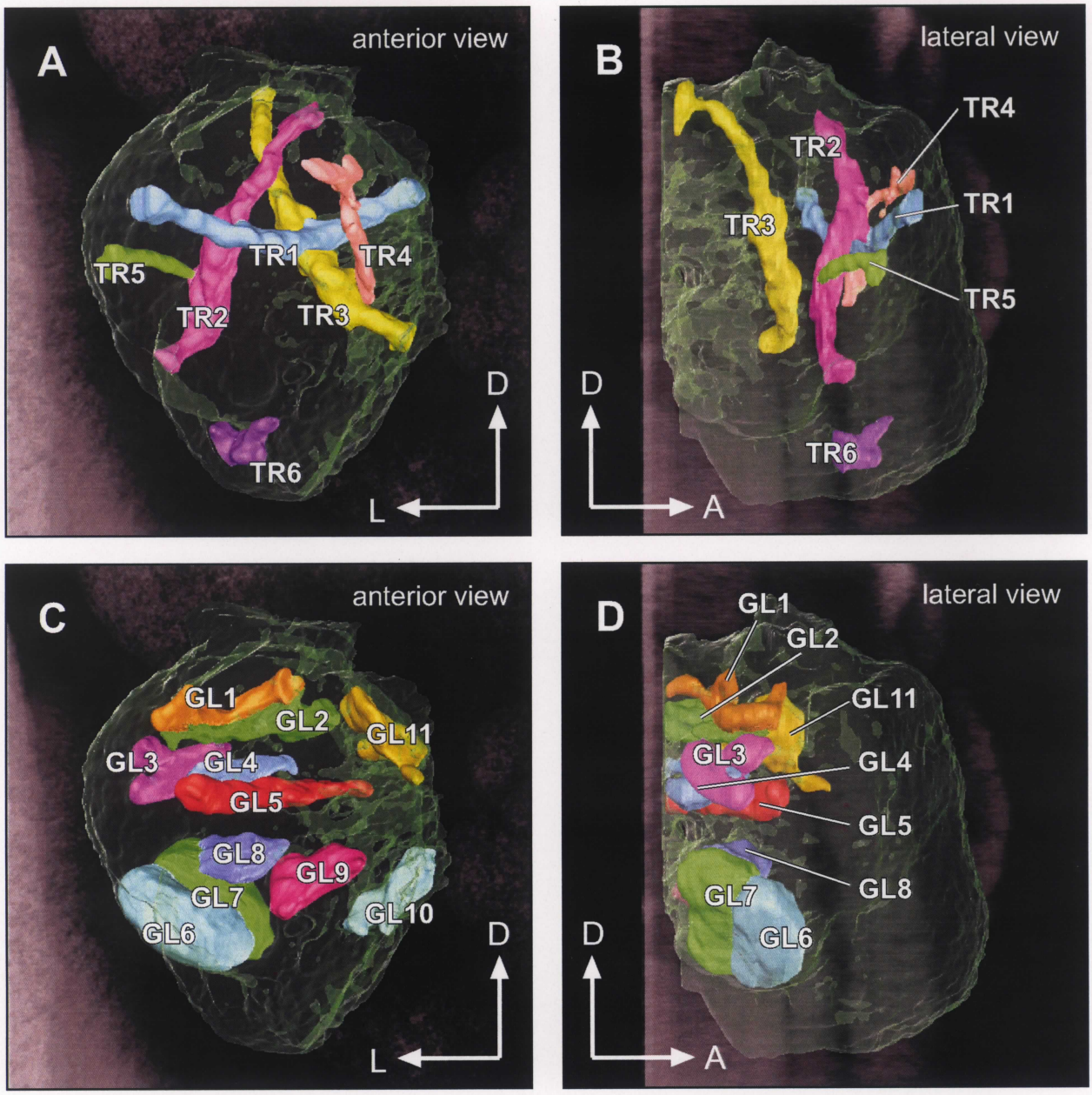

Figure 4. Spatial arrangements of the tracts and the glomeruli in the vlpr.

A, B: Spatial arrangement of the tracts, the anterior view (A) and the lateral view (B). The whole brain was immunostained with nc82 antibody and observed with Zeiss LSM 510. The regions not stained with nc82 were selected on the software Amira 3.1.1 (Mercury Inc.) and reconstructed. All of the tracts are connected to the outer surface of the vlpr, where the cell bodies of neurons reside. TR1, TR2 and TR3 run across the vlpr and project to other neuropile areas, whereas TR4, TR5 and TR6 end within the vlpr.

C, D: Spatial arrangement of the neuropile, the anterior view (C) and the lateral view (D). The strongly labeled areas within the vlpr were determined as glomeruli. The whole vlpr and the glomeruli were reconstructed. All of the eleven glomeruli were located on the posterior half of the neuropile.

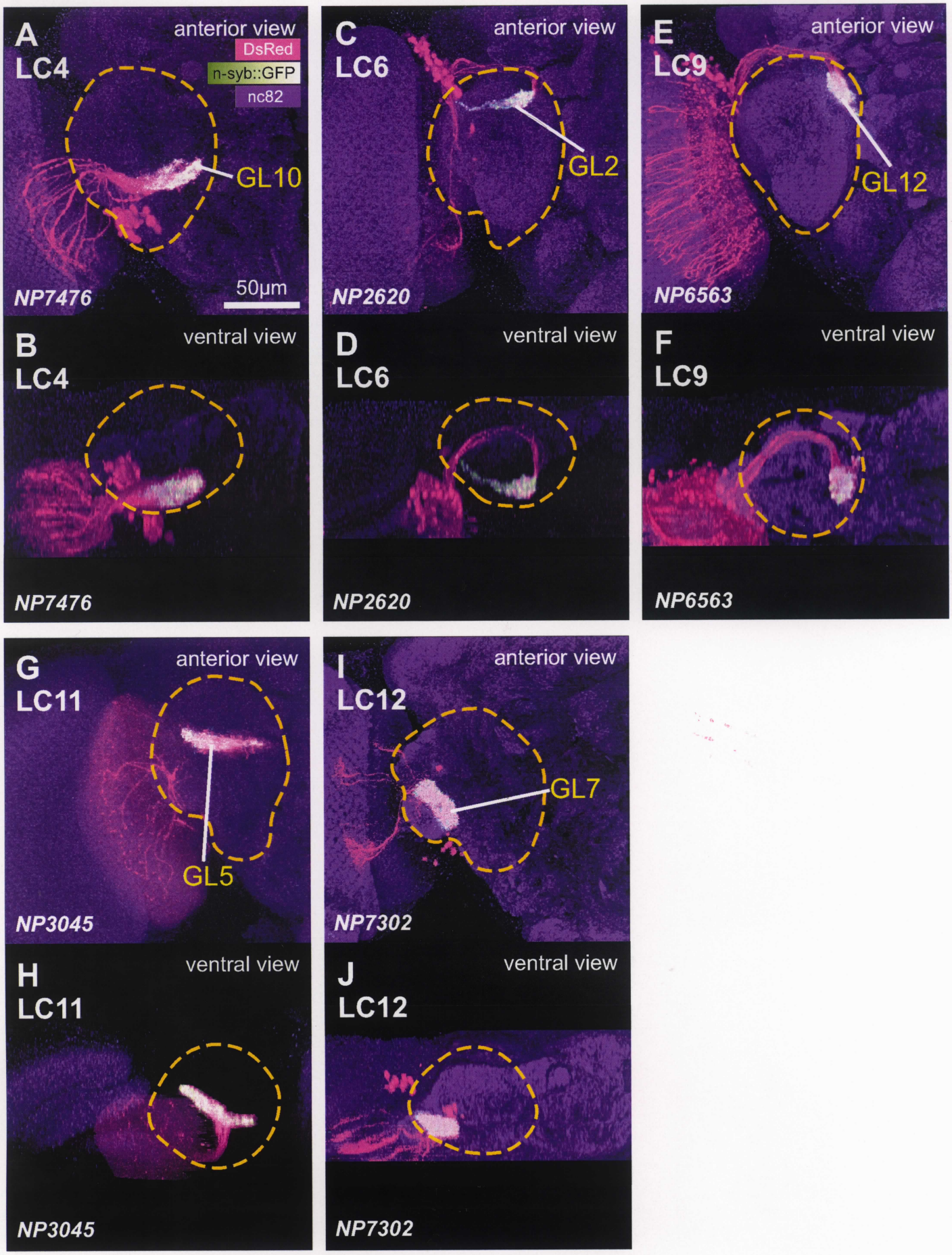

Figure 5. The lobula-specific columnar-type visual pathways.

A, C, E, G, I: anterior view; B, D, F, H, J: ventral view. Dashed yellow lines indicate the outer contour of the vlpr. Projected images were reconstructed with Imaris 2.7.

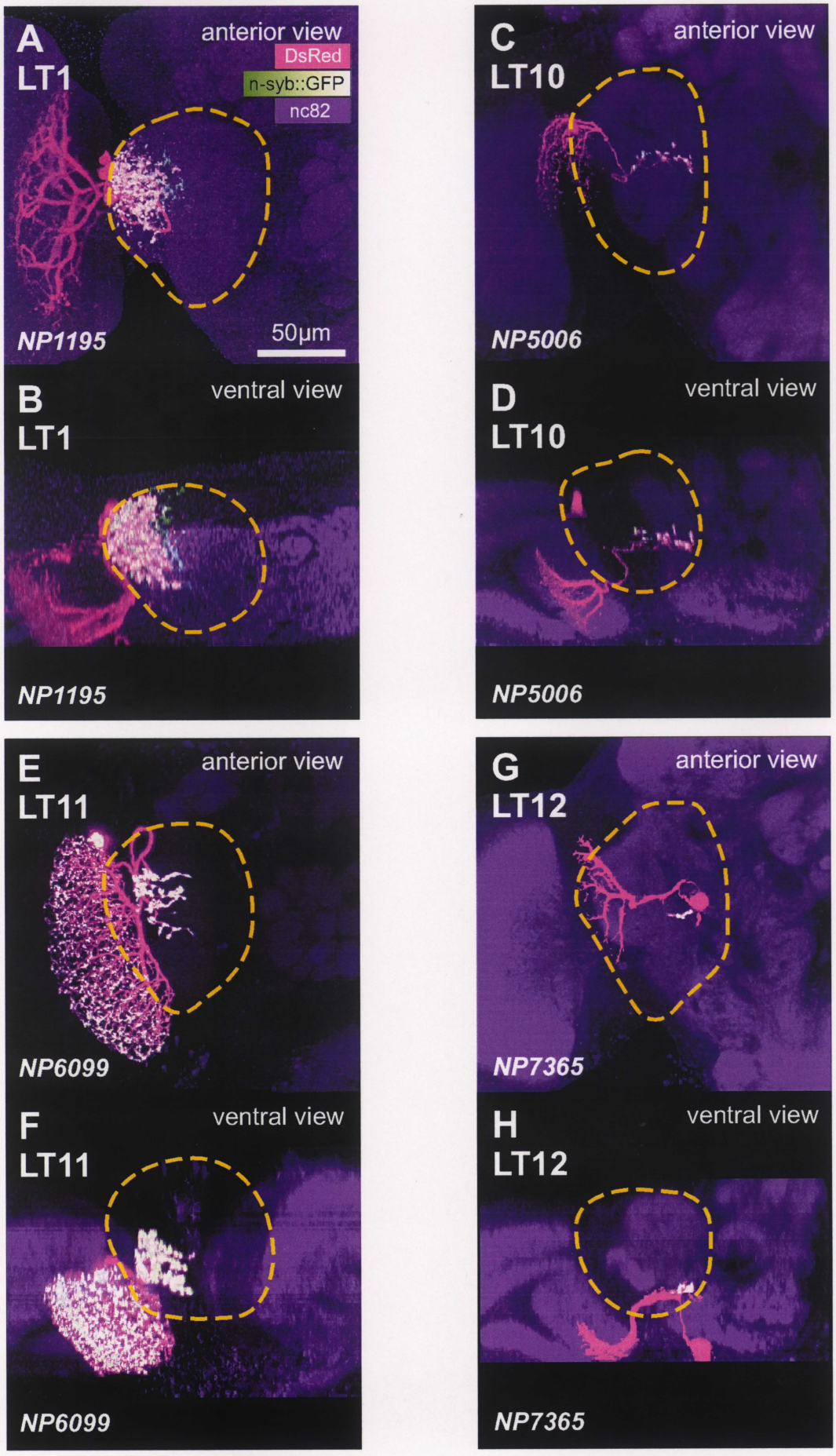

Figure 6. The lobula-specific tangential/tree-like visual pathways.

A, C, E, G: anterior view; B, D, F, H: ventral view. Dashed yellow lines indicate the outer contour of the vlpr. Projected images were reconstructed with Imaris 2.7.

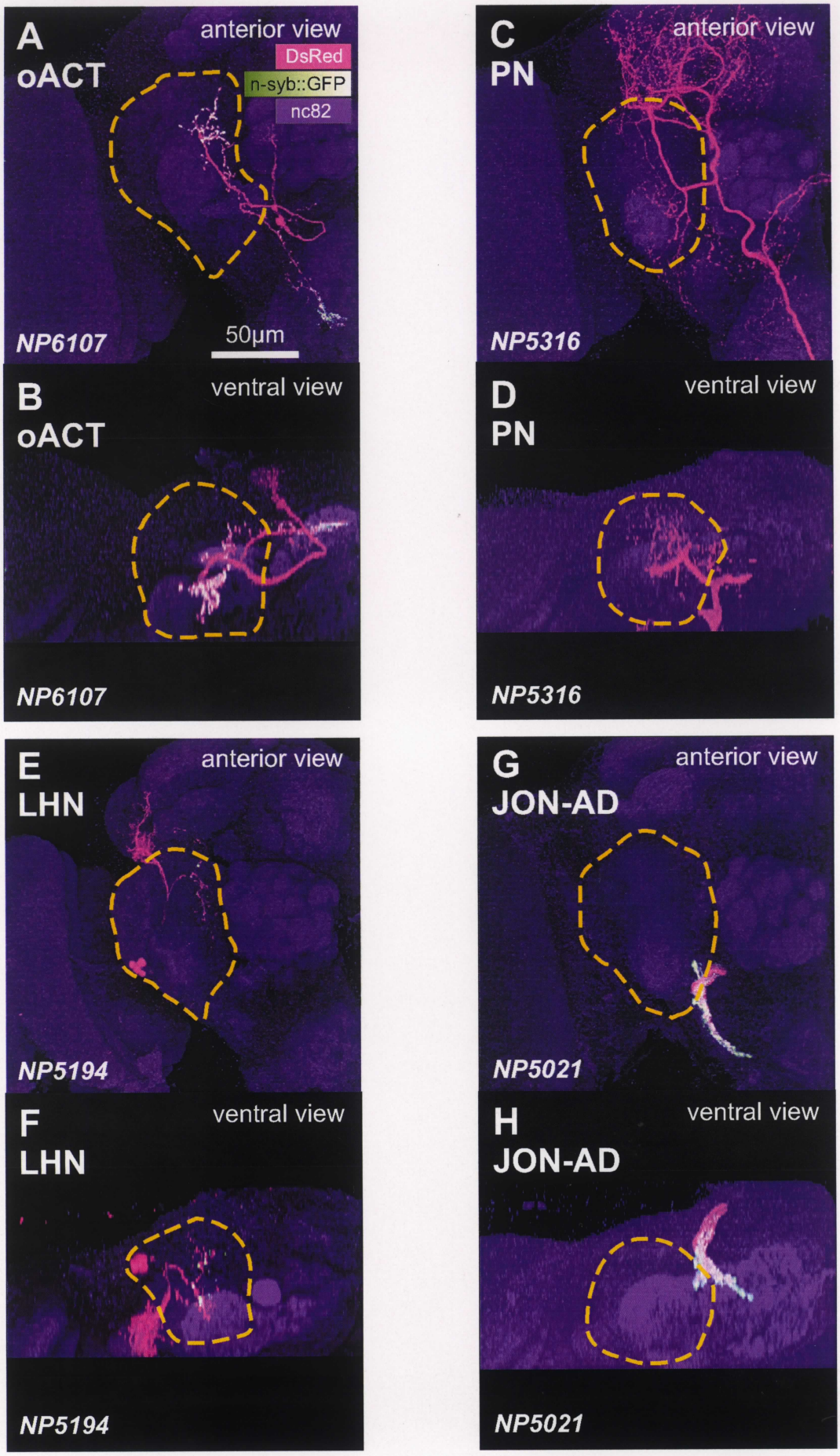

Figure 7. The olfactory pathways (A-F) and the auditory pathway (G, H).

A, C, E, G: anterior view; B, D, F, H: ventral view. Dashed yellow lines indicate the outer contour of the vlpr. Projected images were reconstructed with Imaris 2.7.

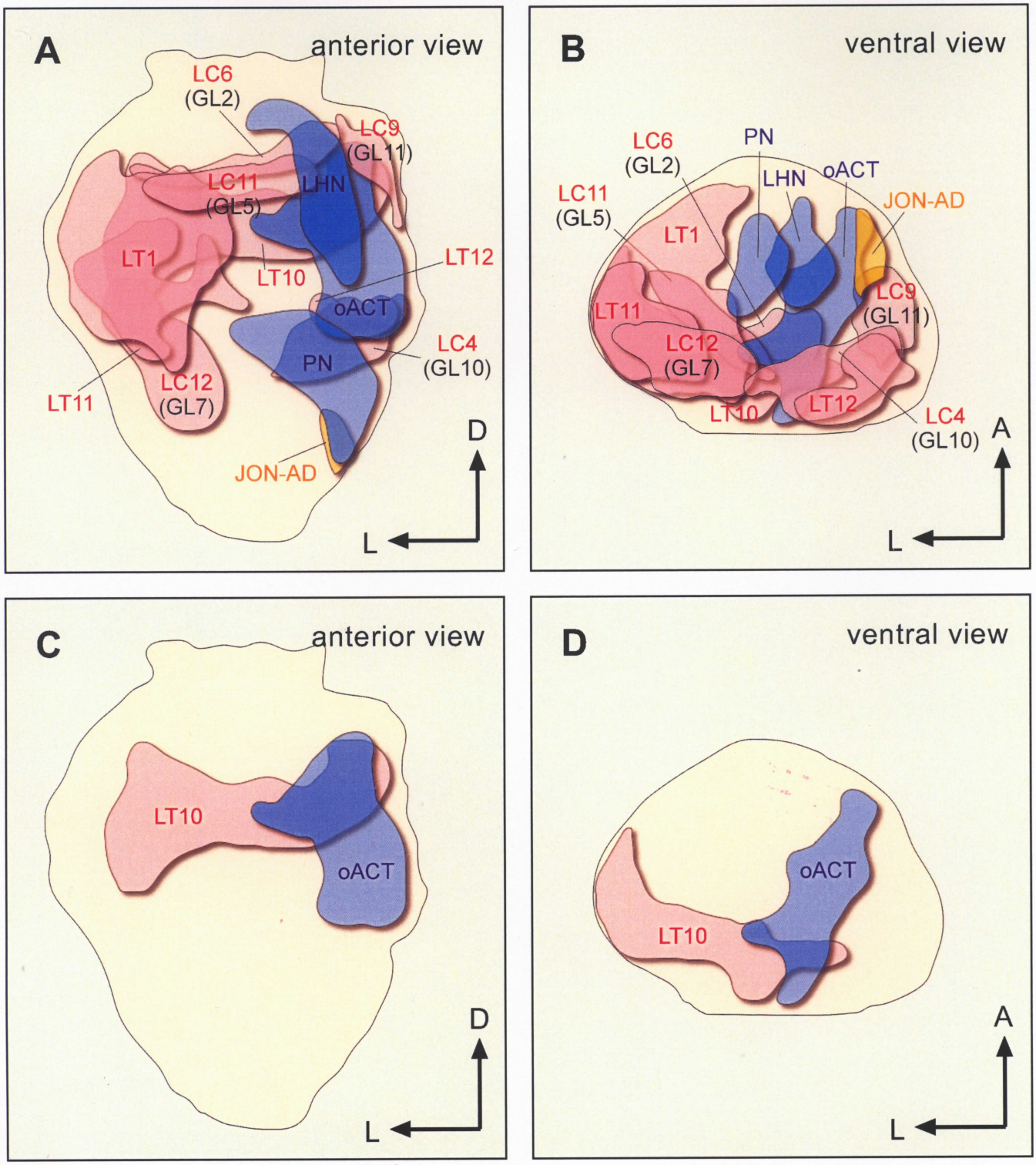

Figure 8. Target regions of the sensory pathways in the vlpr.

A, B: Schematic views of the target regions of thirteen sensory pathways, the anterior view (A) and the ventral view. Pink: visual pathways, Blue: olfactory pathways, Yellow: auditory pathway. Projection sites of different modalities are largely separated from each other.

C, D: Only two projection sites of different modalities that may overlap. The LT10 is a tangential type visual pathway and the oACT is an olfactory pathway. The two pathways could be connected directly, though presence of synapses between them is not yet confirmed.

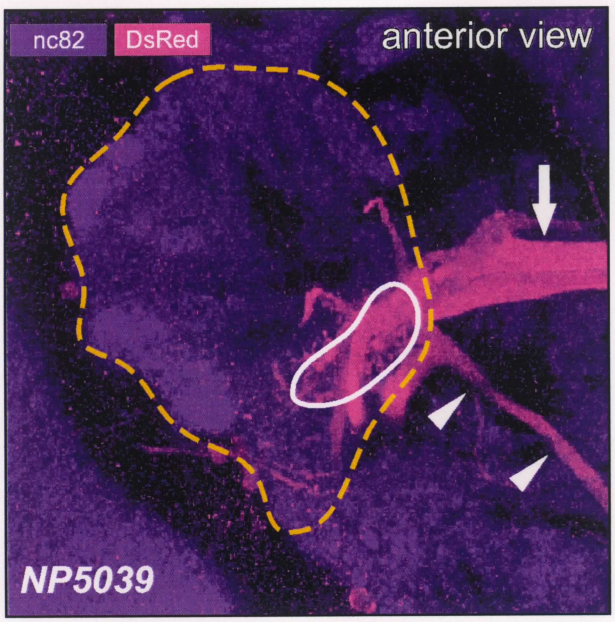

Figure 9. Projection of the giant fiber to the GL10.

The giant fiber is a prominent descending neuron that connects the protocerebrum and the thoracic ganglia. The giant fiber is known to have both electric and chemical synapses with a visual projection pathway called colA in the lateral protocerebrum. Here nc82 immunostaining was applied with the GAL4 enhancer-trap line *NP5039*, which labels the giant fiber system. The terminal of the giant fiber in the vlpr innervates the GL10, the presynaptic terminal of the LC4 visual pathway. Dashed yellow line: contour of the vlpr, white line: GL10, arrowheads: axon of the giant fiber, arrow: the commissure of optic foci.

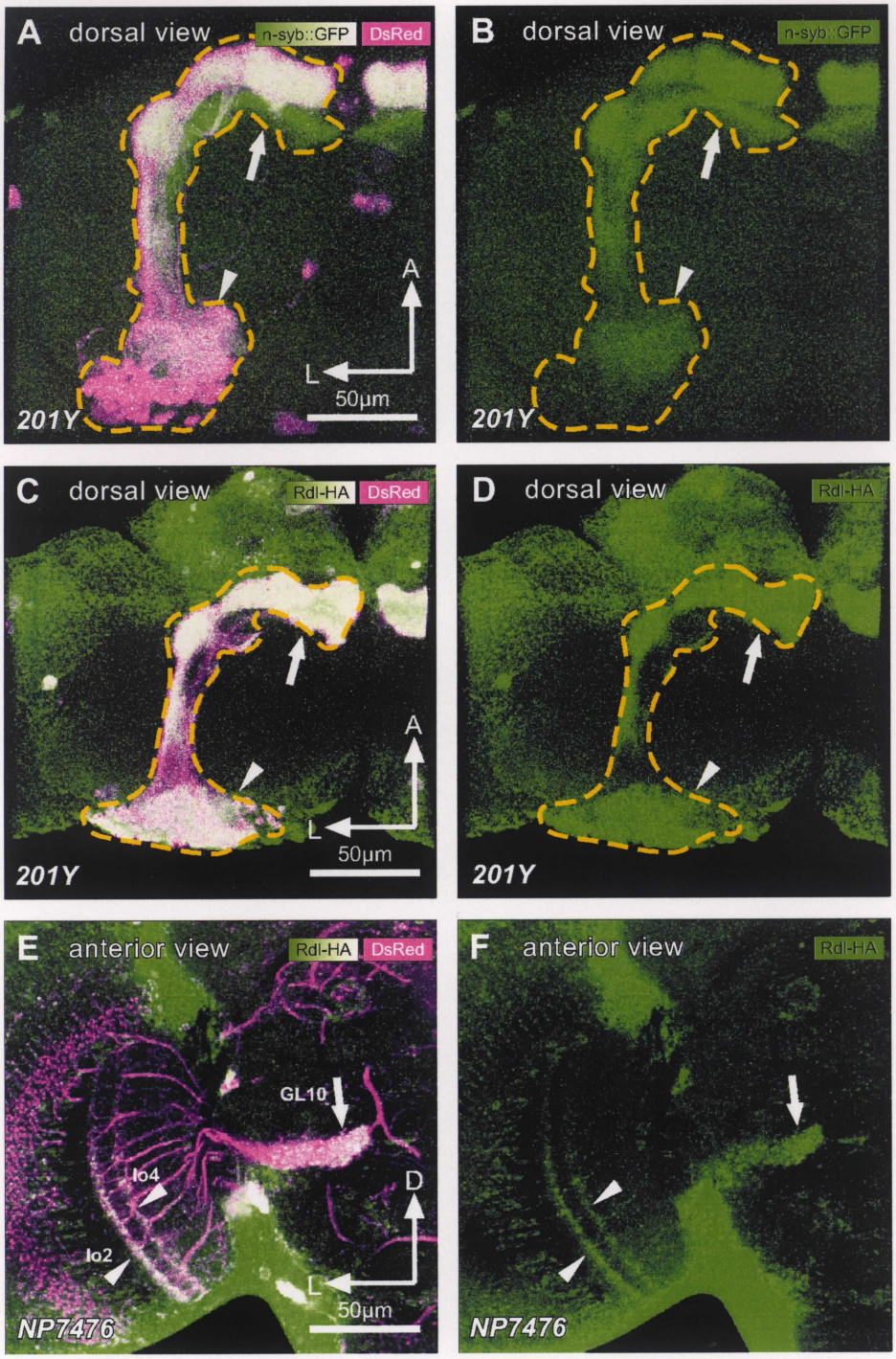

Figure 10. Localization of n-syb::GFP and Rdl-HA.

A: DsRed (purple) and n-syb::GFP (green) driven by *201Y* GAL4, which specifically labels the mushroom body. n-syb::GFP is localized in the lobes (arrow), but not in the calyx (arrowhead).

B: DsRed (purple) and Rdl-HA (green) driven by *201Y* GAL4. In contrast to n-syb::GFP, Rdl-HA is localized both in the lobes and calyx.

C, D: DsRed (purple) and Rdl-HA (green) driven by *NP7476* (LC4). Rdl-HA is localized in the layers in the lobula (arrowheads) and in the glomerulus (arrow). Only the Rdl-HA channel is displayed in D. Compare with the localization pattern of n-syb::GFP in the same pathway (Fig. 5A).

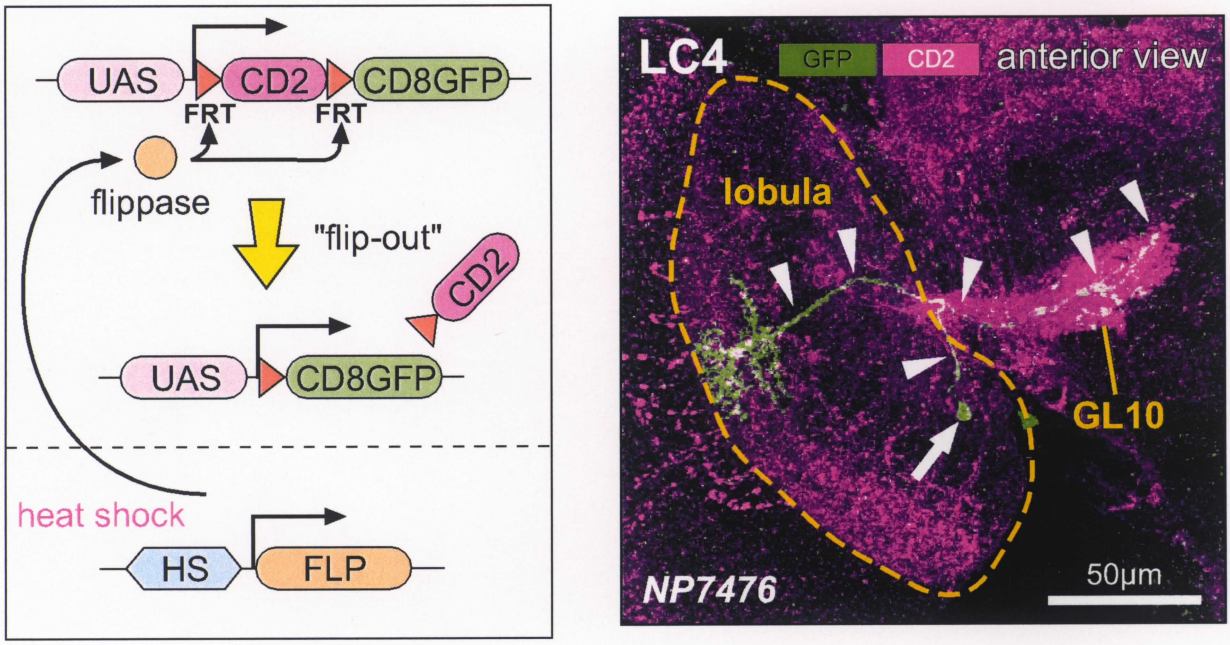

Figure 11. Single cell labeling by flip-out system.

To observe finer structures within the sensory pathways, a combined method of GAL4 enhancer-trap and flip-out system (flippase/FRT system) was applied. Flip-out system enables the visualizing of only a small subset of the GAL4-expressing cells. Expression of the FLP (flippase recombinase) gene after a heat-shock promoter depends on a heat shock. Flippase cuts off the region between the FRT (flippase recognition target) sequences. In this experiment (left), the CD2 gene is driven by GAL4 in absence of flippase, while mCD8::GFP on downstream of the CD2 is expressed only when the CD2 is removed by flippase. Even a single cell can be labeled with GFP if the heat shock is weak enough. LC4 is applied in this study as a typical multi-neuronal pathway in this study (right). Arrow: cell body of the labeled neuron with GFP, arrowheads: axon and cell body fiber.

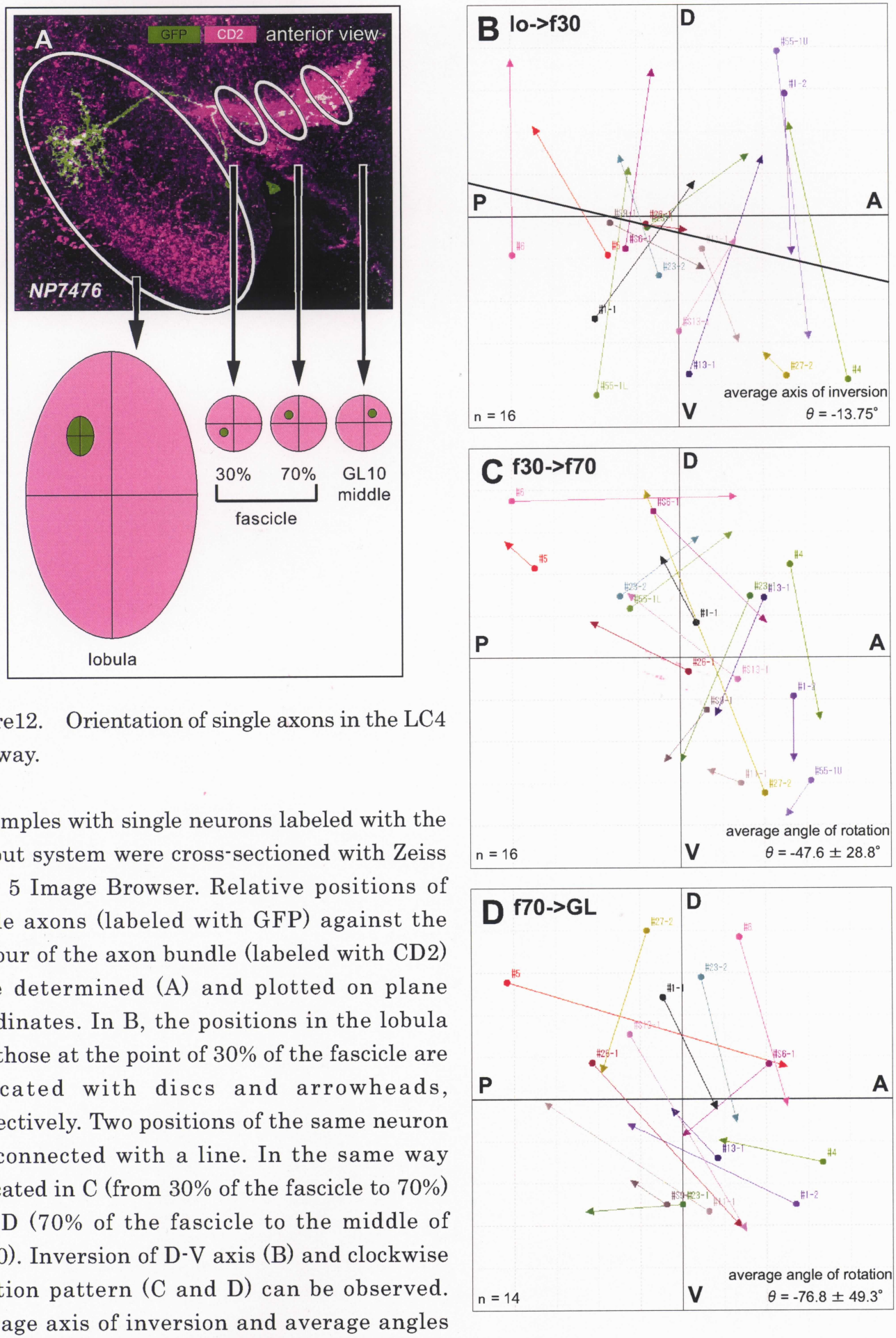

Figure12. Orientation of single axons in the LC4 pathway.

Samples with single neurons labeled with the flip-out system were cross-sectioned with Zeiss LSM 5 Image Browser. Relative positions of single axons (labeled with GFP) against the contour of the axon bundle (labeled with CD2) were determined (A) and plotted on plane coordinates. In B, the positions in the lobula and those at the point of 30% of the fascicle are indicated with discs and arrowheads, respectively. Two positions of the same neuron are connected with a line. In the same way indicated in C (from 30% of the fascicle to 70%) and D (70% of the fascicle to the middle of GL10). Inversion of D-V axis (B) and clockwise rotation pattern (C and D) can be observed. Average axis of inversion and average angles of rotation are indicated in the diagrams.

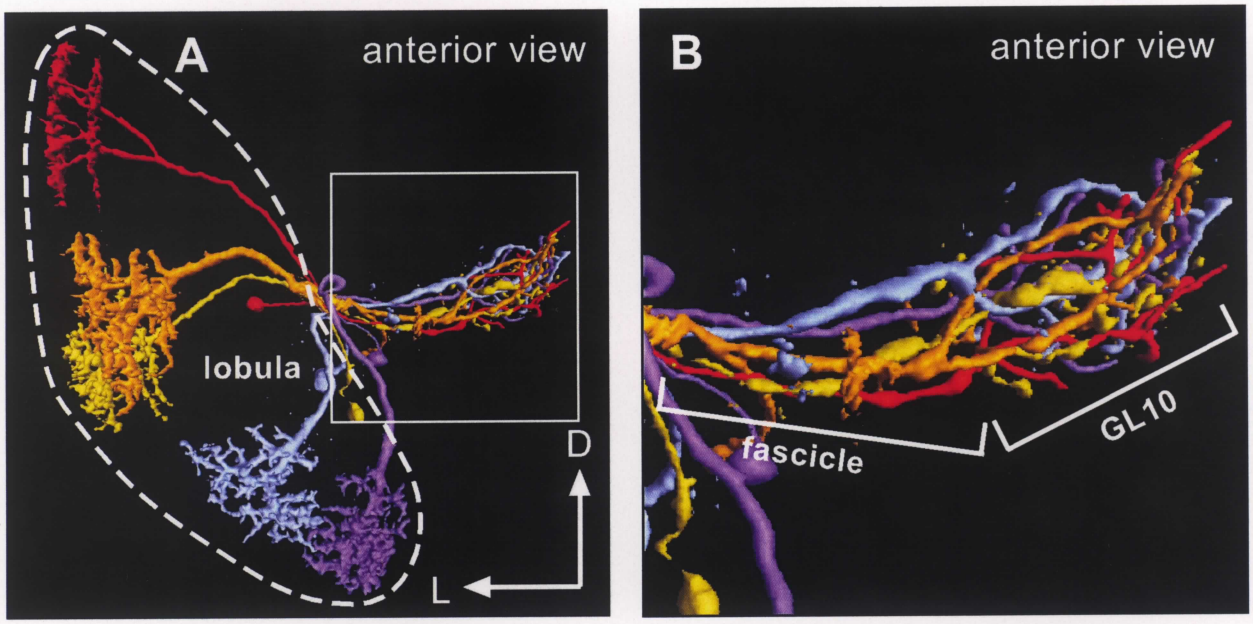

Figure 13. Spatial orientation of the neurons of LC4.

Five LC4 neurons were collected from five independent samples and standardized into one brain with Amira 3.1.1 using the VIB (Virtual Insect Brain) method. Whole pathway (A), and magnification of fascicle and GL10 (B). Twisted pattern of the axons and intermingled structure in the glomeruli are observed.

modality		pathway	GAL4		cell body site	cell number	lower-order sites	projection		
			strain	chrom.	(D/V-A/P)			n-syb::GFP sites		Rdl-HA sites
								neuropiles	within vlpr	
VISUAL	columnar	LC4	*NP7476*	3	LCBR (m-P)	27±2	lo2, 4	vlpr	**GL10**	**GL10**, lo2, 4
		LC6	*NP2620*	2	LCBR (D-m)	approx. 330	lo3, 4, 5, 6	vlpr	**GL2**	**GL2**, lo?
		LC9	*NP6563*	3	LCBR (D-m)	approx. 90±10	lo3, 4, 5?, 6?	vlpr	**GL11**	**GL11**, lo5?, 6?
		LC11	*NP3045*	2	LCBR (D-P)	38±2	lo2, 3, 4	vlpr	**GL5**	**GL5**, lo2
		LC12	*NP7302*	n.d.	LCBR (m-A)	32.5±2.5	lo3, 4	vlpr	**GL7**	**GL7**, lo?
	tangential /tree-like	LT1	*NP1195*	2	LCBR (D-m)	4	lo3	vlpr	**DL**	n.d.
		LT10	*NP5006*	X	LCBR (D-m)	1	lo4	vlpr	**VA**	n.d.
		LT11	*NP6099*	X	LCBR (D-m)	1	lo3, 4, 5	lo3, 4, vlpr	**P-DL**	n.d.
		LT12	*NP7365*	2	LCBR (m-P)	1	lo4	vlpr	**VM**	n.d.
OLFACTORY		oACT	*NP6107*	X	AL ventral	1	7 of ALgl	ammc, vlpr	**P-DM**	n.d.
		PN	*NP5316*	3	calyx ventral	1	14 of ALgl	c.c, slpr, smpr, SOG, vlpr	**VA**	n.d.
		LHN	*NP5194*	2	LCBR (m-A)	12.3±1.5	LH	vlpr	**DM**	n.d.
AUDITORY		JON-AD	*NP5021*	X	JO (D-l)	n.d.	(JO)	vlpr	**VM**	**VM**

Table 1. GAL4 enhancer-trap strains that label pathways projecting to the vlpr.

The thirteen sensory pathways and GAL4 strains used for labeling them. Projection sites in the vlpr, indicated in bold letters, were analyzed in detail in this study. LCBR: lateral cell body region, AL: antennal lobe, JO: Johnston's organ, lo: lobula, gl: glomeruli, LH: lateral horn, ammc: antennal mechanosensory motor center, c.c.: cervical connection, slpr: superior-lateral protocerebrum, smpr: superior-medial protocerebrum, SOG: suboesophagal ganglion.

The cell body sites within the LCBR and the JO, and the projection sites within the vlpr are indicated with following letters; D/V, L/M, A/P, m (middle region of the